clustering, current seismicity rates, and the rate of $M \geq 6$ events after the first year (Fig. 2D). Among sequences sampled that were consistent with New Madrid early clustering behavior and current seismicity rates, the mean number of $M \geq 6$ earthquakes from 1 year to 200 years post-mainshock was 135. At best, at some points in ETAS phase space ~1.7% of the sequences are consistent with our criteria. Results using a stricter criteria that includes the observation that no $M \geq 6$ earthquakes occurred in the region in the past 100 years (table S1) show that we can reject the long-lived aftershock hypothesis at even higher confidence.

Based on our statistical analysis, the hypothesis that current seismicity in the New Madrid region is primarily composed of aftershocks from the 1811–1812 sequence fails. This is because a sequence active enough at late times to produce the seismicity rates observed today and active enough at early times to produce the short-term clustering observed in the first few months would be highly likely to produce too many aftershocks in the intermediate times. If current seismicity in the New Madrid region is not composed predominantly of aftershocks, there must be continuing strain accrual. This is in agreement with recent work finding nonzero strain measurements in the region that are consistent with ongoing interseismic slip of about 4 mm/year (*21*), in contrast to earlier studies [e.g., (*22*)]. The spatial distribution of the stress pattern driven by this model would be generally consistent with the stress change caused by an earthquake on the Reelfoot fault. This could explain how ongoing microseismicity is not part of an aftershock sequence but is still consistent with the predicted stress change associated with the 1811–1812 sequence (*23*). If ongoing microseismicity does result from ongoing strain accrual, this suggests that the region, along with the neighboring Wabash Valley where nonzero strain has also been observed (*24*), will continue to be a source of hazard.

### References and Notes


1. H. K. Gupta, N. P. Rao, B. K. Rastogi, D. Sarkar, *Science* **291**, 2101–2102 (2001).
2. S. E. Hough, M. Page, *J. Geophys. Res.* **116**, (B3), B03311 (2011).
3. A. C. Johnston, *Geophys. J. Int.* **126**, 314–344 (1996).
4. O. W. Nuttli, *Bull. Seismol. Soc. Am.* **63**, 227 (1973).
5. S. E. Hough, *Seismol. Res. Lett.* **80**, 1045–1053 (2009).
6. J. E. Ebel, K.-P. Bonjer, M. C. Oncescu, *Seismol. Res. Lett.* **71**, 283–294 (2000).
7. S. Stein, M. Liu, *Nature* **462**, 87–89 (2009).
8. F. Omori, *J. Coll. Sci. Imp. Univ. Tokyo* **7**, 111 (1895).
9. T. Utsu, *Geophys. Mag.* **30**, 521 (1961).
10. T. Utsu, Y. Ogata, R. S. Matsu'ura, *J. Phys. Earth* **43**, 1–33 (1995).
11. Y. Ogata, *J. Am. Stat. Assoc.* **83**, 9–27 (1988).
12. K. R. Felzer, R. E. Abercrombie, G. Ekstršm, *Bull. Seismol. Soc. Am.* **94**, 88–98 (2004).
13. Y. Ogata, *J. Geophys. Res.* **97**, (B13), 19845 (1992).
14. M. C. Gerstenberger, D. A. Rhoades, *Pure Appl. Geophys.* **167**, 877–892 (2010).
15. Y. Ogata, J. Zhuang, *Tectonophysics* **413**, 13–23 (2006).
16. A. L. Llenos, J. J. McGuire, Y. Ogata, *Earth Planet. Sci. Lett.* **281**, 59–69 (2009).
17. W. H. Bakun, M. G. Hopper, *Bull. Seismol. Soc. Am.* **94**, 64–75 (2004).
18. M. P. Tuttle, *Bull. Seismol. Soc. Am.* **92**, 2080–2089 (2002).
19. K. J. Coppersmith *et al*., Central and Eastern United States Seismic Source Characterization for Nuclear Facilities Project, Technical Report (Electric Power Research Institute, Palo Alto, CA, 2012).
20. S. E. Hough, *Bull. Seismol. Soc. Am.* **103**, 2767 (2013).
21. A. Frankel, R. Smalley, J. Paul, *Bull. Seismol. Soc. Am.* **102**, 479–489 (2012).
22. E. Calais, J. Y. Han, C. DeMets, J. M. Nocquet, *J. Geophys. Res.* **111**, (B6), 6402 (2006).
23. K. Mueller, S. E. Hough, R. Bilham, *Nature* **429**, 284–288 (2004).
24. G. A. Galgana, M. W. Hamburger, *Seismol. Res. Lett.* **81**, 699–714 (2010).
25. K. R. Felzer, R. E. Abercrombie, G. Ekström, *Bull. Seismol. Soc. Am.* **93**, 1433–1448 (2003).



**Acknowledgments:** We thank J. Hardebeck, C. Mueller, and two anonymous reviewers for comments on the manuscript. The CEUS-SSC catalog is available at: www.ceus-ssc.com/Report/Downloads.html. Author Contributions: M.T.P. did the ETAS modeling, and S.E.H. provided expertise on the historical catalog. Both authors participated in the writing.


### Supplementary Materials

www.sciencemag.org/content/343/6172/762/suppl/DC1
Materials and Methods
Fig. S1
Table S1
References (*26*–*30*)


7 November 2013; accepted 15 January 2014
Published online 23 January 2014;
10.1126/science.1248215


# Evolutionarily Dynamic Alternative Splicing of *GPR56* Regulates Regional Cerebral Cortical Patterning


**Byoung-Il Bae,[1]* Ian Tietjen,[1]*† Kutay D. Atabay,[1] Gilad D. Evrony,[1] Matthew B. Johnson,[1] Ebenezer Asare,[1] Peter P. Wang,[1] Ayako Y. Murayama,[2] Kiho Im,[3] Steven N. Lisgo,[4] Lynne Overman,[4] Nenad Šestan,[5] Bernard S. Chang,[6] A. James Barkovich,[7] P. Ellen Grant,[3] Meral Topçu,[8] Jeffrey Politsky,[9]‡ Hideyuki Okano,[2] Xianhua Piao,[10] Christopher A. Walsh[1]§**



The human neocortex has numerous specialized functional areas whose formation is poorly understood. Here, we describe a 15–base pair deletion mutation in a regulatory element of *GPR56* that selectively disrupts human cortex surrounding the Sylvian fissure bilaterally including "Broca's area," the primary language area, by disrupting regional *GPR56* expression and blocking RFX transcription factor binding. *GPR56* encodes a heterotrimeric guanine nucleotide–binding protein (G protein)–coupled receptor required for normal cortical development and is expressed in cortical progenitor cells. GPR56 expression levels regulate progenitor proliferation. *GPR56* splice forms are highly variable between mice and humans, and the regulatory element of gyrencephalic mammals directs restricted lateral cortical expression. Our data reveal a mechanism by which control of *GPR56* expression pattern by multiple alternative promoters can influence stem cell proliferation, gyral patterning, and, potentially, neocortex evolution.


Although most mammals have elaborate and species-specific patterns of folds ("gyri") in the neocortex, the genetic and evolutionary mechanisms of cortical gyrification are poorly understood (*1*–*3*). Abnormal gyrification, such as polymicrogyria (too many small gyri), invariably signals abnormal cortical development, so regional disorders of gyrification are of particular interest, because they highlight mechanisms specific to cortical regions. The human cortex contains dozens of cortical regions specialized for distinct functions—such as language, hearing, and sensation—yet it is unsolved how these cortical regions form and how human cortical regions evolved from those of prehuman ancestors.

Examination of >1000 individuals with gyral abnormalities identified five individuals from three


[1]Division of Genetics and Genomics, Manton Center for Orphan Disease, and Howard Hughes Medical Institute, Boston Children's Hospital, Broad Institute of MIT and Harvard, and Departments of Pediatrics and Neurology, Harvard Medical School, Boston, MA 02115, USA. [2]Department of Physiology, Keio University School of Medicine, Tokyo 160-8582, Japan. [3]Division of Newborn Medicine, Center for Fetal Neonatal Neuroimaging and Developmental Science, Department of Radiology, Boston Children's Hospital, Harvard Medical School, Boston, MA 02115, USA. [4]The MRC-Wellcome Trust Human Developmental Biology Resource (HDBR), Newcastle, Institute of Genetic Medicine, International Centre for Life, Central Parkway, Newcastle upon Tyne NE1 3BZ, UK. [5]Department of Neurobiology and Kavli Institute of Neuroscience, Yale University School of Medicine, New Haven, CT 06520, USA. [6]Beth Israel Deaconess Medical Center, Comprehensive Epilepsy Center, Boston, MA 02215, USA. [7]Departments of Radiology, Pediatrics, Neurology, and Neurological Surgery, University of California San Francisco, San Francisco, CA 94143, USA. [8]Department of Pediatrics, Hacettepe University Faculty of Medicine, Ankara, Turkey. [9]Department of Neurology, Medical College of Georgia, Augusta, GA 30912, USA. [10]Division of Newborn Medicine, Boston Children's Hospital and Harvard Medical School, Boston, MA 02115, USA.

*The authors contributed equally to this work.
†Present address: Department of Anesthesiology, Pharmacology and Therapeutics, University of British Columbia, Vancouver, British Columbia V6T 1Z4, Canada.
‡Present address: Northeast Regional Epilepsy Group, Atlantic Neuroscience Institute Epilepsy Center, Summit, NJ 07901, USA.
§Corresponding author. E-mail: christopher.walsh@childrens.harvard.edu

families (one Turkish and two Irish-American) with strikingly restricted polymicrogyria limited to the cortex surrounding the Sylvian fissure (Fig. 1, A and B; fig. S1; and movies S1 and S2), which suggests a rare, but genetically distinctive, condition. Affected individuals suffered intellectual and language difficulty, as well as refractory seizures (onset 7 months to 10 years), but had no motor disability (table S1). Magnetic resonance imaging (MRI) and quantitative gyral analysis showed abnormal inferior and middle gyri in prefrontal and motor cortex, with mildly affected temporal lobes. Broca's area—the "motor center for speech" (*4*)—in the left hemisphere and the corresponding areas of the right hemisphere were most severely affected. Affected neocortical surface showed abnormally numerous, small gyral-like folds that fused in coarse, irregular patterns, with abnormal and highly irregular white matter protrusions, consistent with polymicrogyria (*5*, *6*), along with widening of the Sylvian fissure (Fig. 1A and fig. S1B).

Genome-wide analysis identified a single linked locus on chromosome 16q12.2-21 (Fig. 1C) containing the *GPR56* gene, which, when mutated in its coding region, leads to polymicrogyria of the entire neocortex, as well as cerebellar and white matter abnormalities (*7*–*9*). As we found no mutations in the exons of *GPR56*, we sequenced 38 conserved non-exonic elements (table S2), in one of which we identified a small deletion in all five individuals. The mutated element normally contains two copies of a 15–base pair (bp) tandem repeat, but all affected individuals have a homozygous deletion of one 15-bp repeat (Fig. 1, E and F). The deletion is heterozygous in parents of the affected individuals, who manifest no obvious clinical signs, and is absent from thousands of control chromosomes in the Single-Nucleotide Polymorphism Database and 1000 Genomes database. The two Irish-American families carry the mutation on the same chromosomal haplotype, which reflects a common founder. It is noteworthy that the Turkish family carries the same deletion on a distinct haplotype, which indicates that the mutation arose independently (Fig. 1D). The element is located <150 bp upstream of the transcriptional start site of noncoding exon 1m (e1m) of *GPR56*, which suggests that it may regulate e1m expression as a cis-regulatory element. *GPR56* has at least 17 alternative transcription start sites, each beginning from a different noncoding first exon; all of the start sites are predicted to drive transcription of mRNAs whose coding sequence starts from exon 3 (Fig. 2A and fig. S2A) and all of which encode the same GPR56 protein (*10*, *11*). The diverse noncoding first exons have distinct expression profiles, with e1m being the most robustly transcribed first exon in fetal human brain but with several other alternative transcripts also expressed in fetal and adult brain (Fig. 2A and fig. S2, B to D).

To confirm that the 15-bp deletion disrupts perisylvian *GPR56* expression, we generated transgenic mice with the 23-kb human *GPR56* upstream region driving green fluorescent protein (GFP) expression. The 23-kb region encompasses 16 of the 17 transcription start sites containing e1m and ends before the translation start codon (Fig. 2A). This construct drives GFP expression in the entire central nervous system, including neocortex, and recapitulates the location and relative amount of expression of endogenous mouse GPR56 protein (Fig. 2B and fig. S3). In contrast, the 23-kb construct containing the 15-bp deletion drives expression in medial, but not lateral, cortex or lateral ganglionic eminence (Fig. 2B). These data suggest that the cis-regulatory element upstream of e1m drives *GPR56* expression in the perisylvian and lateral cortex, whereas disruption of the element, with consequent impairment of e1m expression, causes the perisylvian malformation.

To elucidate how the 15-bp deletion in the cis-regulatory element disrupts e1m expression,

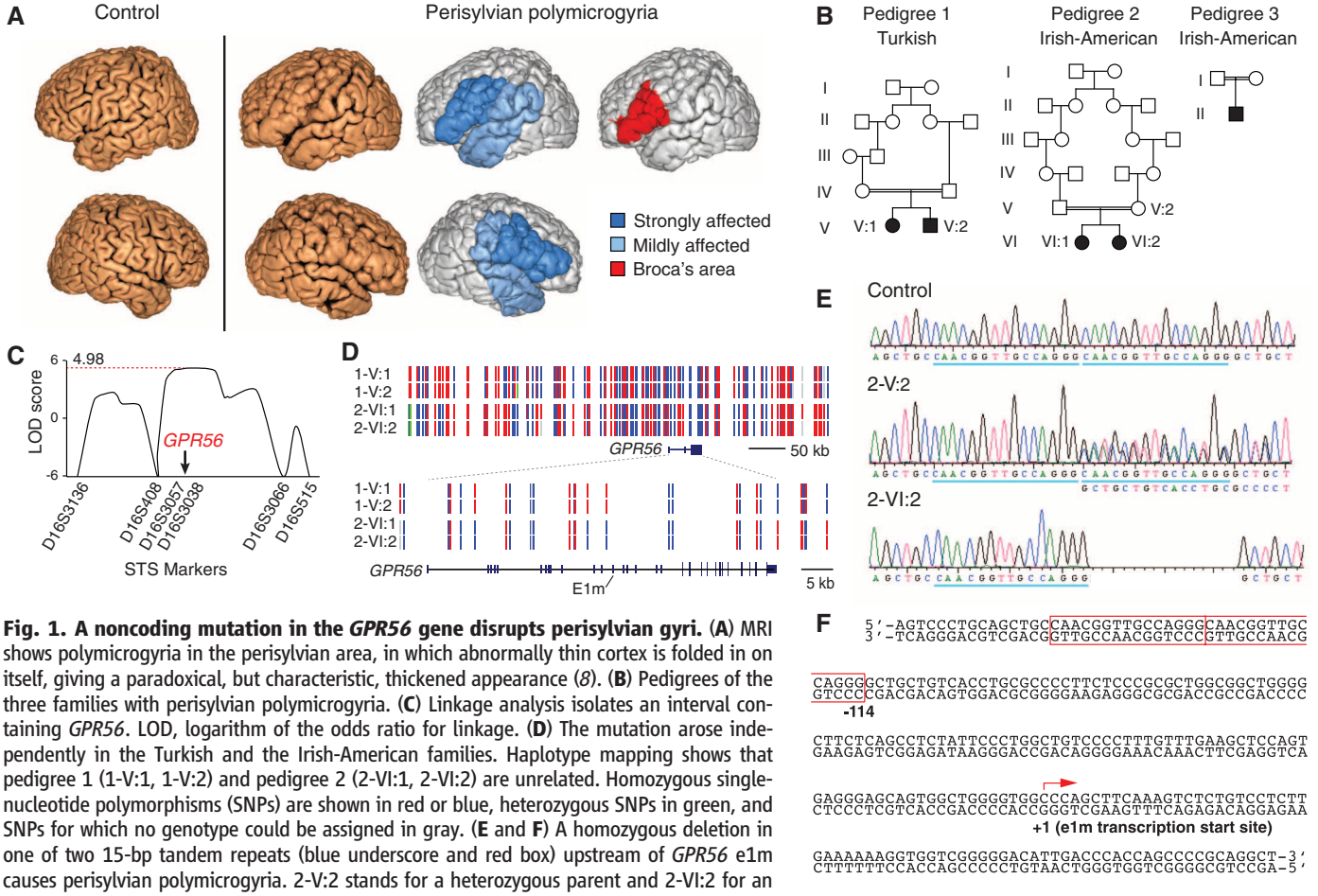


**Fig. 1. A noncoding mutation in the *GPR56* gene disrupts perisylvian gyri.** (**A**) MRI shows polymicrogyria in the perisylvian area, in which abnormally thin cortex is folded in on itself, giving a paradoxical, but characteristic, thickened appearance (*8*). (**B**) Pedigrees of the three families with perisylvian polymicrogyria. (**C**) Linkage analysis isolates an interval containing *GPR56*. LOD, logarithm of the odds ratio for linkage. (**D**) The mutation arose independently in the Turkish and the Irish-American families. Haplotype mapping shows that pedigree 1 (1-V:1, 1-V:2) and pedigree 2 (2-VI:1, 2-VI:2) are unrelated. Homozygous single-nucleotide polymorphisms (SNPs) are shown in red or blue, heterozygous SNPs in green, and SNPs for which no genotype could be assigned in gray. (**E** and **F**) A homozygous deletion in one of two 15-bp tandem repeats (blue underscore and red box) upstream of *GPR56* e1m causes perisylvian polymicrogyria. 2-V:2 stands for a heterozygous parent and 2-VI:2 for an affected individual from pedigree 2.

we performed yeast one-hybrid (Y1H) screening of a mouse forebrain cDNA library with the human cis-regulatory element as bait and obtained multiple yeast colonies encoding members of the *regulatory factor X (Rfx)* transcription factor family (Fig. 2C) (*12*). RFX1 and RFX3 bind the normal element in vitro, with binding decreased 60 to 70% by the 15-bp deletion (Fig. 2D). Chromatin immunoprecipitation sequencing confirmed RFX3 binding to the element (fig. S4) (*13*). RFX1 and GPR56 colocalize in germinal zones of fetal human brain (Fig. 2E). Dominant-negative RFX abrogates normal, but not mutant, e1m promoter activity on embryonic day 13.5 (E13.5) in mouse cortical cultures (Fig. 2F). Furthermore, genetic ablation of *Rfx4* decreases *Gpr56* expression in developing mouse brain (*14*). *RFX* and *GPR56* expression patterns are correlated (fig. S5, A and B) (*15*), with *RFX3* and *RFX7* most prominent in human ventrolateral prefrontal cortex, the region affected in perisylvian polymicrogyria (Fig. 2G), which suggests that multiple RFX proteins regulate the element.

*GPR56* encodes an adhesion heterotrimeric guanine nucleotide–binding protein (G protein)–coupled receptor that is highly expressed in cortical progenitors (*7*, *16*) and binds extracellular matrix proteins (*17*). Loss of *GPR56* disrupts radial glia and causes breaches in the pial basement membrane, through which some neurons overmigrate (*9*, *16*). However, even where the pia is intact, we found that neocortical thickness and organization are irregular, with occasional thin regions in *Gpr56* knockout mice (Fig. 3A). Postmortem analysis of a human with biallelic *GPR56* coding mutations showed a very thin cortex, which suggested potential roles of *GPR56* in neurogenesis as well (*9*). GPR56 protein is most highly expressed in progenitors in the ventricular and subventricular zones during neurogenesis in mice (*16*, *18*). GPR56 expression in developing human and marmoset neocortex is highest in the ventricular zone, as well as in the outer subventricular zone, which is expanded in mammals with larger brains (*2*) (Fig. 3B and fig. S5, C and D).

Impairment and overexpression of *GPR56* show that its expression regulates proliferation. *Gpr56* knockout mice show fewer phosphohistone H3 (PH3)–positive mitotic progenitor cells and TBR2-positive intermediate progenitors than wild-type mice in the neocortex at E14.5. Conversely, mice carrying a transgene that directs overexpression of human *GPR56* show increased

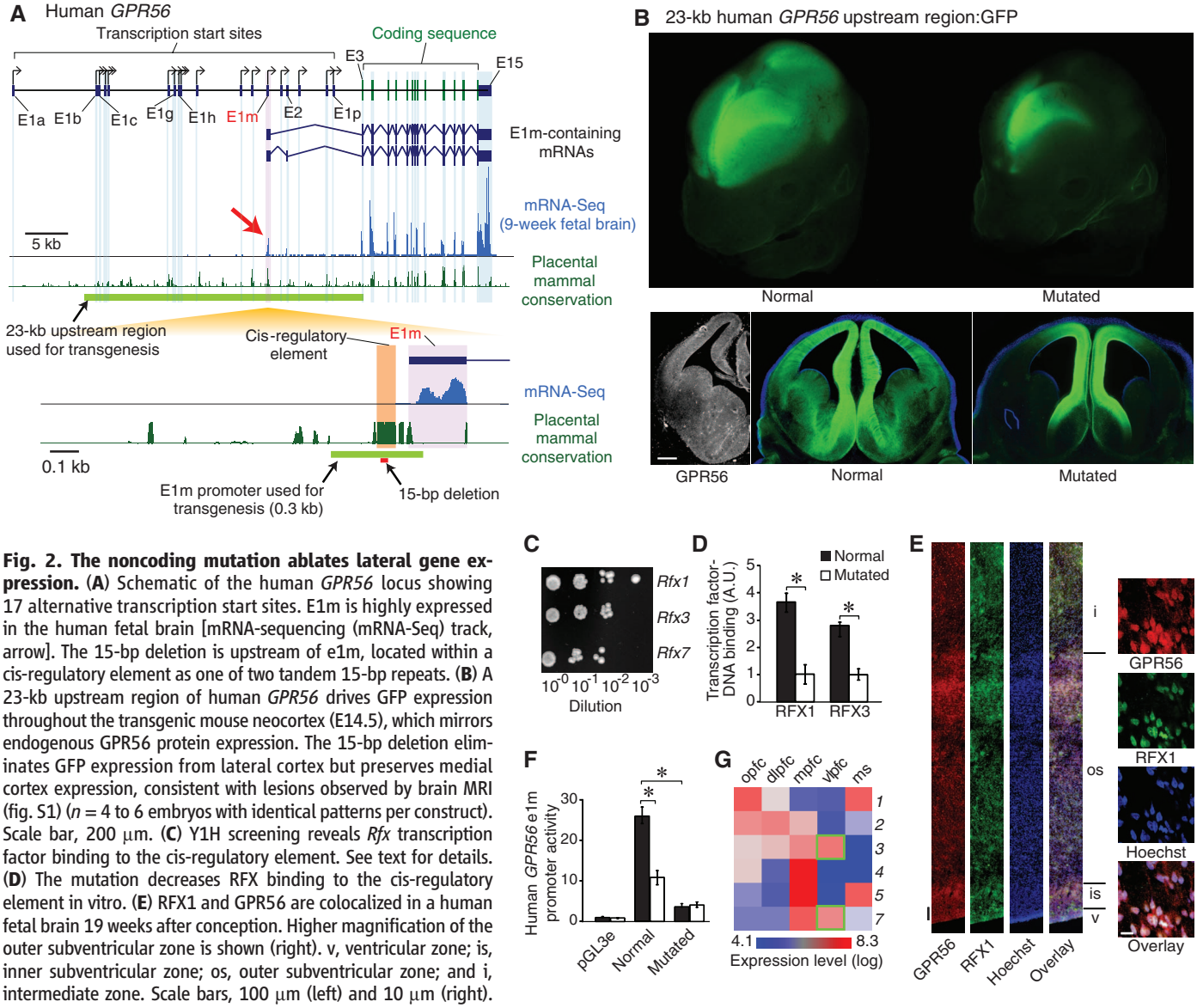


**Fig. 2. The noncoding mutation ablates lateral gene expression.** (**A**) Schematic of the human *GPR56* locus showing 17 alternative transcription start sites. E1m is highly expressed in the human fetal brain [mRNA-sequencing (mRNA-Seq) track, arrow]. The 15-bp deletion is upstream of e1m, located within a cis-regulatory element as one of two tandem 15-bp repeats. (**B**) A 23-kb upstream region of human *GPR56* drives GFP expression throughout the transgenic mouse neocortex (E14.5), which mirrors endogenous GPR56 protein expression. The 15-bp deletion eliminates GFP expression from lateral cortex but preserves medial cortex expression, consistent with lesions observed by brain MRI (fig. S1) ($n = 4$ to 6 embryos with identical patterns per construct). Scale bar, 200 μm. (**C**) Y1H screening reveals *Rfx* transcription factor binding to the cis-regulatory element. See text for details. (**D**) The mutation decreases RFX binding to the cis-regulatory element in vitro. (**E**) RFX1 and GPR56 are colocalized in a human fetal brain 19 weeks after conception. Higher magnification of the outer subventricular zone is shown (right). v, ventricular zone; is, inner subventricular zone; os, outer subventricular zone; and i, intermediate zone. Scale bars, 100 μm (left) and 10 μm (right). (**F**) Dominant-negative RFX (white bars) abrogates normal e1m promoter activity. Black bars, GFP control. (**G**) Each *RFX* gene has distinct expression patterns in the fetal human brain. Each number means the corresponding *RFX* isoform. *RFX3* and *RFX7* are enriched in regions affected by perisylvian polymicrogyria (green boxes). pfc, prefrontal cortex; opfc, orbital pfc; dlpfc, dorsolateral pfc, mpfc, medial pfc; vlpfc, ventrolateral pfc; ms, motor-sensory cortex. *$P < 0.001$, *t* test.

mitotic progenitor cells and intermediate progenitor cells (Fig. 3, C and D). In utero electroporation (at E13.5 with analysis 48 hours later at E15.5) of a plasmid encoding *GPR56* (as well as GFP, to mark the cells) caused cells to persist in proliferative zones compared with cells expressing GFP alone (Fig. 3E). Changes in the number of intermediate progenitors in transgenic and knockout mice may be secondary to changes in the radial progenitor cells that generate them or might reflect a direct role of GPR56 in intermediate progenitors but is consistent with a report that loss of *TBR2* (*EOMES*) also causes polymicrogyria in humans (*19*).

The cis-regulatory element upstream of *GPR56* e1m is found in genomes of all placental mammals, but not monotremes, marsupials, or nonmammals, which suggests that it emerged after placental and nonplacental mammals diverged 85 to 100 million years ago (fig. S7B). The cis-regulatory element sequence is only found at the e1m locus in *GPR56* but not elsewhere in the genome. E1m itself shows homology at its 3′ end to a long interspersed nuclear element (LINE)–4/RTE, a family of retrotransposons active in early mammals after divergence from marsupials (*20*). Another noncoding *GPR56* exon (exon 2), present only in primates, derives from a primate-specific *Alu* insertion (fig. S7B). In contrast to the >17 alternative first exons in humans, we found only five noncoding first exons in the mouse *Gpr56* gene (Fig. 4A and fig. S7A) (*10*, *11*). Thus, *GPR56* acquired many noncoding upstream exons and generated alternative splice forms with distinct expression patterns (fig. S2, B and D), in the lineage leading to humans. Transposable element insertion played a role in generating this diversity.

To test directly whether evolutionary changes in *GPR56*'s alternative splice forms have functional effects, we generated transgenic mice in which the β-galactosidase (β-gal) gene is driven by a minimal 300-bp e1m promoter from human, mouse, marmoset, dolphin, and cat (Fig. 2A and fig. S6A). The mouse e1m promoter drives β-gal expression broadly in the nervous system in diverse cell types, which suggests that this simple 300-bp e1m promoter is sufficient to recapitulate major features of the endogenous mouse GPR56 expression (*16*–*18*) (Fig. 4B and fig. S6B). In contrast, the corresponding human e1m promoter has a variety of deletions and single-nucleotide variants, relative to the mouse sequence (fig. S6A), and drives much more limited expression in rostral-lateral cortex (Fig. 4B and fig. S6B). Weak lateral cortical expression is visible in embryos carrying the mouse e1m promoter:β-gal transgene,

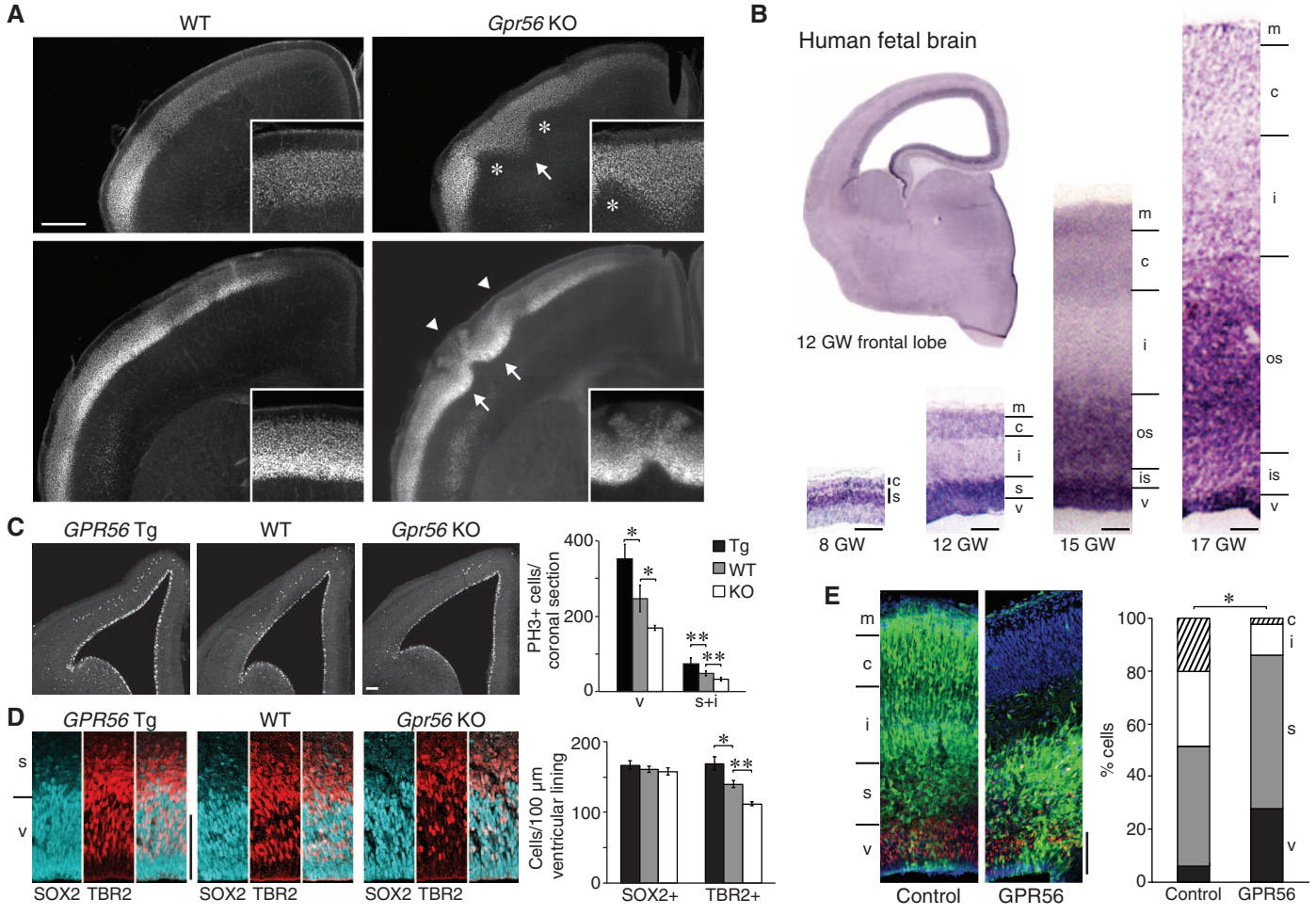


**Fig. 3. GPR56 regulates neuroprogenitor proliferation.** (**A**) In *Gpr56* knockout mice, neurons overmigrate through breached pial basement membrane (arrowheads) or undermigrate (arrows) forming irregular cortical layers, as shown by immunostaining of Cux1, an upper layer (II to IV) marker (p9). Thin cortex is occasionally observed (asterisks). (**B**) *GPR56* is highly expressed in human ventricular zone and outer subventricular zone at 12 to 17 weeks of gestation (GW), which suggests roles in neuroprogenitors. v, ventricular zone; s, subventricular zone; is, inner subventricular zone; os, outer subventricular zone; i, intermediate zone; c, cortical plate; and m, marginal zone. (**C** to **D**) Human *GPR56* transgenic (Tg) mice have significantly more mitotic (PH3+) neuroprogenitor cells and intermediate progenitor (TBR2+) cells than wild-type (WT). In contrast, *Gpr56* knockout (KO) mice have significantly fewer mitotic cells and intermediate progenitors than WT (E13.5 to E14.5). ($n$ = 7 mice per genotype; *$P$ < 0.005; **$P$ < 0.001; paired $t$ test). (**E**) The cells that are in utero electroporated (from E13.5 to E15.5) with human *GPR56*-IRES-GFP [either side of the internal ribosome entry site (IRES), GFP expressing] persist in the germinal zones longer that the GFP control cells. Red, TBR2; blue, Hoechst. ($n$ = 11 mouse embryos per construct; *$P$ < 0.0001; chi-squared test). Scale bars, 500 μm (A) and 100 μm (B) to (E).

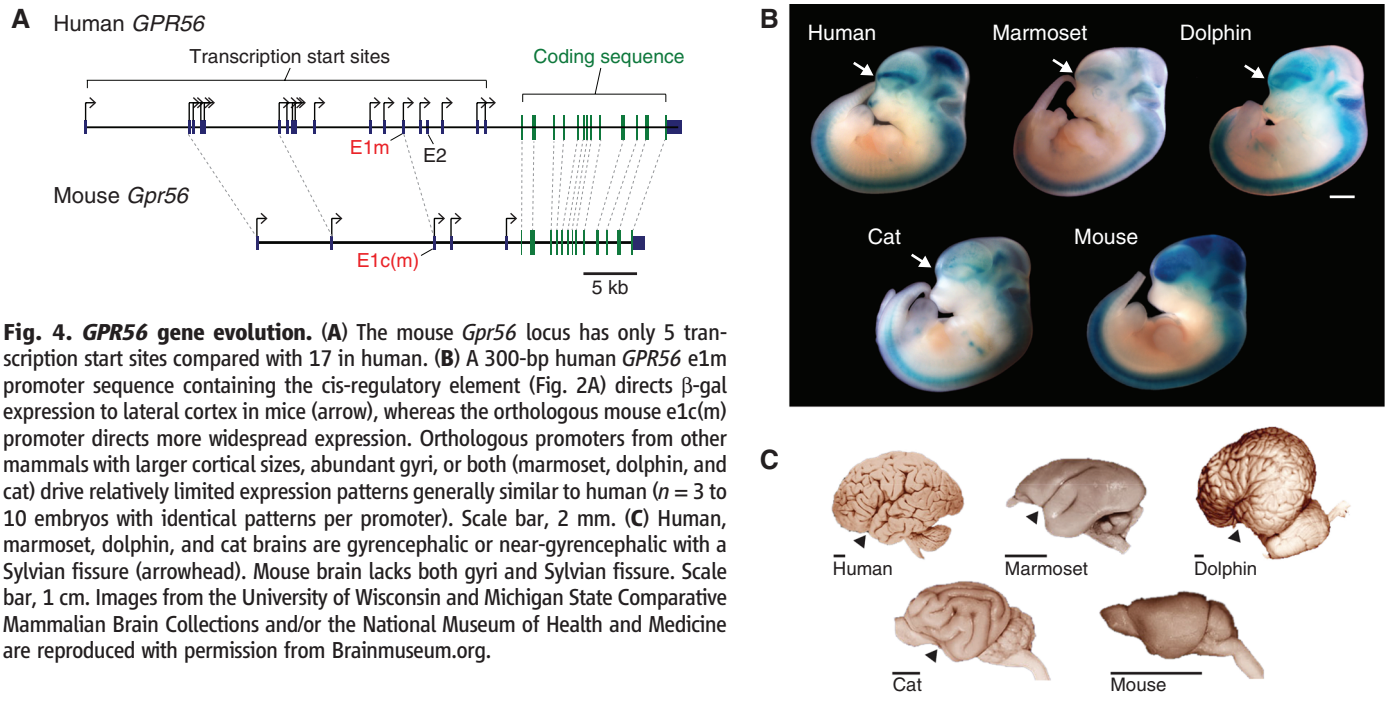


**Fig. 4. *GPR56* gene evolution.** (**A**) The mouse *Gpr56* locus has only 5 transcription start sites compared with 17 in human. (**B**) A 300-bp human *GPR56* e1m promoter sequence containing the cis-regulatory element (Fig. 2A) directs β-gal expression to lateral cortex in mice (arrow), whereas the orthologous mouse e1c(m) promoter directs more widespread expression. Orthologous promoters from other mammals with larger cortical sizes, abundant gyri, or both (marmoset, dolphin, and cat) drive relatively limited expression patterns generally similar to human ($n = 3$ to 10 embryos with identical patterns per promoter). Scale bar, 2 mm. (**C**) Human, marmoset, dolphin, and cat brains are gyrencephalic or near-gyrencephalic with a Sylvian fissure (arrowhead). Mouse brain lacks both gyri and Sylvian fissure. Scale bar, 1 cm. Images from the University of Wisconsin and Michigan State Comparative Mammalian Brain Collections and/or the National Museum of Health and Medicine are reproduced with permission from Brainmuseum.org.

which suggests that, in humans, additional elements besides the 300-bp e1m promoter region are required to drive the full complement of *GPR56* expression. E1m promoters from marmoset, dolphin, and cat drive expression patterns generally similar to human. The shared expression patterns in the four mammals that have a Sylvian fissure (Fig. 4C) suggest that elaboration of *GPR56* noncoding regulation is consistent with the larger number of noncoding first exons in gyrencephalic mammals and humans. Elaboration of additional alternative splice forms provides a mechanism for potentially independent evolution of these multiple forms.

Our studies show that levels of *GPR56* control proliferation of progenitors in the neocortex. Loss of *GPR56* expression impairs neurogenesis, and overexpression enhances proliferation and progenitor number. Selective *GPR56* loss causes strikingly regional defects of cortical development. *GPR56* likely influences progenitor proliferation by stabilizing the basal process of radial neuroepithelial progenitors, because (i) GPR56 protein localizes to the basal processes of radial neuroepithelial cells (*16*); (ii) GPR56 binds extracellular matrix proteins in the pial basement membrane, such as collagen type III (*17*) and tetraspanins, which bind integrins as well (*21*); (iii) GPR56 is required for normal attachment of basal processes to the pial basement membrane in mice (*16*); and (iv) basal processes regulate progenitor proliferation via integrin signaling (*22*, *23*), and *GPR56* interacts genetically with $\alpha_3\beta_1$ integrin (*24*). The elaboration of the *GPR56* locus in gyrencephalic mammals, and especially humans, to produce many alternative splice forms with diverse expression patterns presents *GPR56* as a key target that could influence the dramatic changes in shape and folding that characterize the forebrain of many mammals. Elaboration and specialization of alternative transcripts with distinct transcription start sites is an evolutionary mechanism that has been difficult to study because of the lack of comprehensive catalogs of RNA splice forms, but continued RNA sequencing studies may soon provide the opportunity to assess its importance systematically.

## References and Notes


1. P. Rakic, *Nat. Rev. Neurosci.* **10**, 724–735 (2009).
2. J. H. Lui, D. V. Hansen, A. R. Kriegstein, *Cell* **146**, 18–36 (2011).
3. K. Zilles, N. Palomero-Gallagher, K. Amunts, *Trends Neurosci.* **36**, 275–284 (2013).
4. K. Amunts *et al.*, *PLOS Biol.* **8**, e1000489 (2010).
5. J. A. Golden, B. N. Harding, *Nat. Rev. Neurol* **6**, 471–472 (2010).
6. A. J. Barkovich, *Neuroradiology* **52**, 479–487 (2010).
7. X. Piao *et al.*, *Science* **303**, 2033–2036 (2004).
8. X. Piao *et al.*, *Ann. Neurol.* **58**, 680–687 (2005).
9. N. Bahi-Buisson *et al.*, *Brain* **133**, 3194–3209 (2010).
10. D. Thierry-Mieg, J. Thierry-Mieg, *Genome Biol.* **7** (suppl. 1), S12–S14 (2006).
11. Y. Suzuki, R. Yamashita, K. Nakai, S. Sugano, *Nucleic Acids Res.* **30**, 328–331 (2002).
12. S. J. Ansley *et al.*, *Nature* **425**, 628–633 (2003).
13. A. Jolma *et al.*, *Genome Res.* **20**, 861–873 (2010).
14. D. Zhang *et al.*, *J. Neurochem.* **98**, 860–875 (2006).
15. H. J. Kang *et al.*, *Nature* **478**, 483–489 (2011).
16. S. Li *et al.*, *J. Neurosci.* **28**, 5817–5826 (2008).
17. R. Luo *et al.*, *Proc. Natl. Acad. Sci. U.S.A.* **108**, 12925–12930 (2011).
18. S. J. Jeong, R. Luo, S. Li, N. Strokes, X. Piao, *J. Comp. Neurol.* **520**, 2930–2940 (2012).
19. L. Baala *et al.*, *Nat. Genet.* **39**, 454–456 (2007).
20. T. S. Mikkelsen *et al.*, *Nature* **447**, 167–177 (2007).
21. L. Xu, R. O. Hynes, *Cell Cycle* **6**, 160–165 (2007).
22. R. Radakovits, C. S. Barros, R. Belvindrah, B. Patton, U. Müller, *J. Neurosci.* **29**, 7694–7705 (2009).
23. S. A. Fietz *et al.*, *Nat. Neurosci.* **13**, 690–699 (2010).
24. S. J. Jeong *et al.*, *PLOS ONE* **8**, e68781 (2013).


**Acknowledgments:** Research performed on samples of human origin was conducted according to protocols approved by participating institutions, including Boston Children's Hospital and Beth Israel Deaconess Medical Center. The human embryonic and fetal material was provided by the Joint Medical Research Council (grant no. G0700089)–Wellcome Trust (grant no. GR082557) Human Developmental Biology Resource (www.hdbr.org) and the National Institute of Child Health and Human Development, NIH, Brain and Tissue Bank at the University of Maryland (contract no. HHSN275200900011C, reference no. NO1-HD-9-0011). *Gpr56* knockout mice are from Genentech. This work was supported by the Strategic Research Program for Brain Sciences and from the Ministry of Education, Culture, Sports, Science and Technology (MEXT) Japan (H.O.); Funding Program for World-Leading Innovative R&D on Science and Technology (FIRST Program) (H.O.); U01MH081896 from National Institute of Mental Health, NIH (N.S.); 2R01NS035129 from National Institute of Neurological Disorders and Stroke, NIH (C.A.W.); and The Paul G. Allen Family Foundation (C.A.W.). Additional funding support listed in supplementary materials. C.A.W. is an investigator of the Howard Hughes Medical Institute. *Gpr56* knockout mice are available from Genentech subject to a Material Transfer Agreement.

## Supplementary Materials

www.sciencemag.org/content/343/6172/764/suppl/DC1
Materials and Methods
Supplementary Text
Figs. S1 to S7
Tables S1 and S2
Movies S1 to S2
References (*25*–*40*)

7 August 2013; accepted 17 December 2013
10.1126/science.1244392